

## Reduction of dislocation density using in situ deposited SiN<sub>x</sub> intermediate layers in AlGaIn/GaN heterostructures grown by MOVPE on SiC substrates

S. Miller<sup>1)</sup>, H.-J. Lugauer<sup>1)</sup>, S. Bader<sup>1)</sup>, G. Brüderl<sup>1)</sup>, U. Strauss<sup>1)</sup>, A. Lell<sup>1)</sup>, V. Härle<sup>1)</sup>, K. Engl<sup>2)</sup>, M. Beer<sup>2)</sup>

1) OSRAM Opto Semiconductors GmbH, Wernerwerkstr. 2, 93049 Regensburg, Germany, 2) Institute for Experimental and Applied Physics, University of Regensburg, Universitätsstr. 31, 93040 Regensburg, Germany

### Abstract

In situ deposited SiN<sub>x</sub> layers have been used in GaN layers grown by MOVPE on SiC substrates to reduce the dislocation density. Growth pressure of the overgrown GaN layers has been varied to study the influence on morphology and defect density. The dislocation density was determined by hot wet chemical etching with phosphoric acid and atomic force microscopy. We found two types of etch pits which were correlated to pure screw and mixed dislocations as well as pure edge type dislocations. Transmission electron microscopy analyses confirm the correlation between etch pit types and dislocation types. With an in situ deposited SiN<sub>x</sub> layer the density of edge dislocations could be reduced by a factor of 10.

### Introduction

GaN based III–V semiconductors are attractive for short wavelength optoelectronic devices. Due to the lack of GaN bulk crystals, it has been necessary to rely on heteroepitaxial growth techniques with commonly used substrates such as silicon carbide, sapphire or silicon. Unfortunately the lattice mismatch between the GaN epitaxial layer and the substrates results in a high dislocation density. For high performance optoelectronic devices such as blue laser diodes with long lifetimes GaN layers with low defect densities are required. The defect density can be reduced with an in situ method by depositing an intermediate SiN<sub>x</sub> layer which fractionally covers the surface. This technique was first described by Haffouz et al. [2] for GaN growth on sapphire. The treatment of the sapphire substrate by a mixture of silane and ammonia induces a three dimensional growth mode at the first stage of the epitaxial GaN layer which is known to reduce the dislocation density [3,7]. The process was also successfully used for GaN growth on Si substrates [4, 5] and SiC substrates [6]. We present further investigations using this technique for defect reduction in epilayers on SiC substrates.

### Experimental Procedure

AlGaIn/GaN layers were epitaxially grown by metallorganic vapor phase epitaxy (MOVPE) in a low pressure MOVPE reactor on silicon carbide (SiC) substrates. Standard precursors including trimethyl–gallium, trimethyl–aluminium for the epitaxial layers and silane and biscyclopentadienyl–magnesium for n– and p–type doping were used. First an AlGaIn buffer layer was deposited on the SiC substrate followed by a 150 nm GaN:Si layer. The GaN:Si surface was treated by a mixture of silane and ammonia at low temperature (T=500 °C) which results in a fractional coverage of the GaN surface with SiN<sub>x</sub>. The overgrowth of the SiN<sub>x</sub> mask can be described as a kind of micro epitaxial lateral overgrowth [3]. As known from ELOG techniques, the lateral growth can be influenced by varying the growth pressure [1]. In the following the influence of reactor pressure on morphology and defect density of the overgrown GaN:Si layers was investigated. Samples were grown at three different growth pressures of 270 mbar, 100 mbar and 70 mbar. V/III ratio was kept constant in all three cases and H<sub>2</sub> was used as carrier gas except in the 70 mbar experiment. Here a 1:1 mixture of H<sub>2</sub> and N<sub>2</sub> as carrier gas was used as N<sub>2</sub> increases the lateral growth mode which is known from ELOG experiments [1]. For all samples in situ reflectometry spectra were recorded during the growth. Fig. 1 (a) shows the reflectivity signal versus time of the sample overgrown with p=270 mbar growth pressure. It can be divided into four different sections. Section I shows the last few oscillations of the GaN:Si layer grown before the SiN<sub>x</sub> treatment. Section II shows the signal while the SiN<sub>x</sub> mask is deposited. In the gray underlayed section III the development of the reflectivity signal after growth start of the overgrown GaN:Si layer can be seen. Overgrowth of the surface, which is now fractionally covered with SiN<sub>x</sub>, leads to an island–like growth mode as described by Tanaka et al. [6]. As a consequence the reflectivity signal drops because of the rough epilayer surface. When the islands start to coalesce the

reflectivity increases and begins to oscillate again. After smoothing of the surface the signal reaches its maximum level as in section I. The growth rate in the section IV at  $p=270$  mbar was  $2,1 \mu\text{m/h}$ , and the layer thickness from the growth start till the complete smoothing of the surface was estimated to be  $770 \text{ nm}$ . In Fig. 1 (b) sections I and II are similar to Fig. 1(a). Section III shows the reflectivity behaviour for a growth pressure of  $100 \text{ mbar}$ . Time needed from overgrowth start until smoothing was  $940 \text{ s}$  and the corresponding layer thickness was  $500 \text{ nm}$ . The sample smoothed faster compared to Fig. 1 (a).

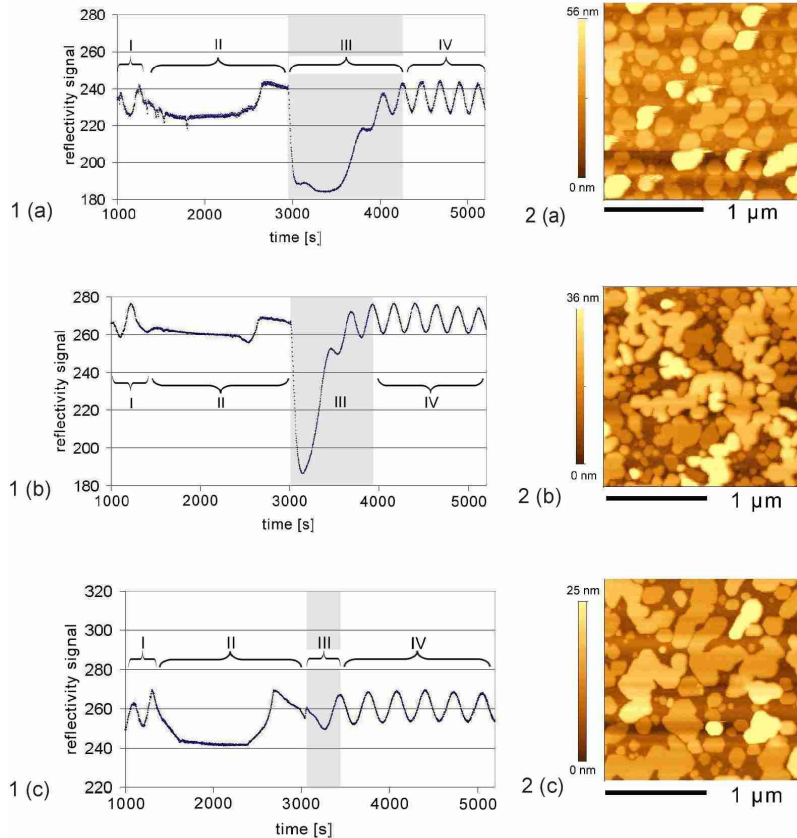


Fig. 1: Reflectometry spectra of samples with an in situ SiN layer overgrown at (a) 270 mbar growth pressure (b) 100 mbar growth pressure (c) 70 mbar growth pressure

Fig. 2: AFM scans of the island growth at a early stage of the overgrowth at (a) 270 mbar growth pressure (b) 100 mbar growth pressure (c) 70 mbar growth pressure

Similar results were found by Figge et al. for the overgrowth of a GaN nucleation layer on sapphire substrates [8]. In the case of  $70 \text{ mbar}$  reactor pressure section III shows the shortest time needed for surface smoothing as can be seen in Fig. 1 (c). The necessary time was  $440 \text{ s}$  and the equivalent layer thickness was  $180 \text{ nm}$ . Compared with Fig. 1 (a) and 1 (b) the reflectivity signal does not drop down very much and starts to oscillate early which indicates a quick smoothing of the surface. In order to investigate the island growth for the three pressure variations, only a thin GaN:Si layer was grown over the  $\text{SiN}_x$  with a nominal thickness of  $10 \text{ nm}$ . The atomic force microscopy (AFM) measurements are depicted in Fig. 2. Fig. 2 (a) shows the sample grown at  $p=270 \text{ mbar}$ . Non-uniform islands can be seen with heights between  $30 \text{ nm}$  and  $60 \text{ nm}$  whereby most of the islands do not show coalescence yet. In the case of the sample with  $p=100 \text{ mbar}$  as depicted in Fig. 2 (b), the coalescence process is more developed and the height of the islands is lower compared with Fig. 2 (a). This indicates a better lateral growth because of the lower growth pressure. The height of most of the islands differs between  $20$  and  $30 \text{ nm}$ . The latter sample depicted in Fig. 2 (c) shows the best lateral growth caused by the low growth pressure of  $70 \text{ mbar}$  and the mixture of carrier gas with  $\text{N}_2$ . The islands are larger compared with the other samples and show partial coalescence which leads to flat surface regions. The height of the structures varies between  $10$  and  $20 \text{ nm}$ . An etch pit density (EPD) method was carried out to determine defect densities following a method published by Visconti et al. [9] for n-type GaN. In our case all samples were capped with a  $100 \text{ nm}$  p-type GaN:Mg layer. The samples were etched one hour with hot phosphoric acid at a temperatur of  $170^\circ \text{ C}$ . The etching process produces a surface,

where dislocations are decorated by etch pits. In Fig. 3 (a) a typical AFM image is shown of an etched sample without any defect reducing procedure. Two kinds of etch pits can be seen.

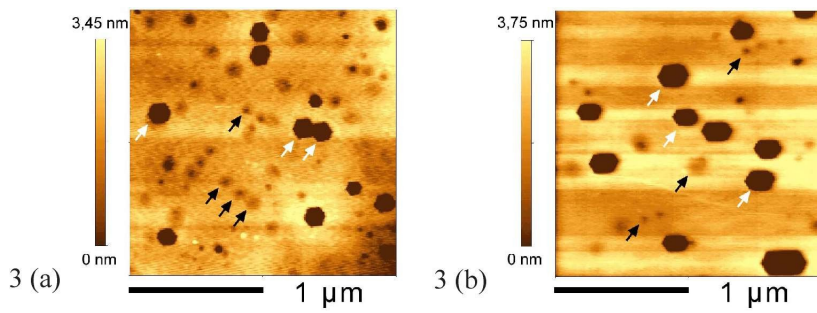
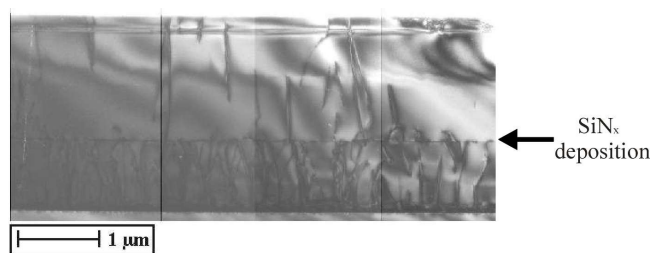


Fig. 3: EPD AFM measurements of a sample (a) without SiN<sub>x</sub> layer (b) with SiN<sub>x</sub> layer

The first type (herein after called type I etch pit) is a well-defined hexagonal etch pit with a depth between 5 nm and 10 nm (marked with white arrows) and a lateral expansion between 100 nm and 250 nm. The type II etch pits (black arrows) have a depth of only 1 nm and a lateral size smaller than 200 nm. For this sample the number of type I and type II etch pits were determined to be  $4 \times 10^8 \text{ cm}^{-2}$  and  $1,3 \times 10^9 \text{ cm}^{-2}$  respectively. As we know from TEM investigations of comparable samples on SiC typical defect densities are in the range of  $4\text{--}5 \times 10^8 \text{ cm}^{-2}$  for screw and mixed dislocations and  $1.5 \times 10^9 \text{ cm}^{-2}$  for edge type dislocations. Considering this fact we relate the type I etch pits to screw and mixed dislocations whereas the smaller type II etch pits correlate with the density of edge type dislocations. In Fig. 3 (b) the EPD measurement of the sample with in situ SiN<sub>x</sub> overgrown at p=100mbar is depicted. The number of type I etch pits and thus the density of the screw and mixed dislocation has not changed very much, whereas the number of type II etch pits has decreased significantly. Screw and mixed dislocation were determined to be in the range of  $3 \times 10^8 \text{ cm}^{-2}$ , whereas edge type dislocations could be reduced to  $4 \times 10^8 \text{ cm}^{-2}$ . Similar measurements were done for the samples with 70 mbar and 270 mbar growth pressure. Screw and mixed dislocations were found to be in the range of  $3\text{--}4 \times 10^8 \text{ cm}^{-2}$  and edge type dislocations in the range of  $3\text{--}4 \times 10^8 \text{ cm}^{-2}$ . A critical remark has to be made concerning the accuracy of this EPD method for an exact determination of the defect density. As the number of etch pits varies more or less dependent from the place where the measurement is done on the sample and dependent of the etching behaviour of the surface an accumulated error of  $\pm 1 \times 10^8 \text{ cm}^{-2}$  has to be taken into account to the measured EPD values. For a better statistic AFM measurements were carried out at several different spots of each sample and based on this we could not observe an influence of the growth pressure on defect reduction although the behaviour of island growth is very different in the early stage of the overgrowth and the influence on the smoothing behaviour is significant.

Fig. 4.: Cross section TEM image of a sample with in situ SiN<sub>x</sub> layer



The samples were further analyzed by transmission electron microscopy (TEM). In Fig.4 a cross section image of the sample grown at 100 mbar is shown. The SiN<sub>x</sub> intermediate layer is clearly visible. A reduction of dislocation density above the SiN<sub>x</sub> layer can be observed as several dislocations are terminated at this layer. The comparison of bright field and dark field weak beam images reveal that mainly edge type dislocations could be reduced which is consistent with the results of our EPD measurements. To confirm the relation between etch pit types and dislocation types cross section TEM images of threading dislocations were made, which end in such etch pits. Fig. 5 (b) shows a bright field image of four dislocations. Three of them end in a type I etch pit (white arrows) whereas at the end of one threading dislocation (black arrow) no etch pit can be seen. Enlarged images of the etch pits are

depicted in Fig. 6 (a) and 6 (b). Their lateral dimensions are 150 nm and 160 nm respectively with a depth of 10 nm. In Fig. 5 (a) a weak beam dark field image of the same region as in Fig. 5 (b) is shown. Here only the three dislocations with the type I etch pits (white arrows) can be seen. The bragg diffraction condition was  $\mathbf{g}=\{0002\}$  which only makes screw and mixed dislocations visible. This is in agreement with our assumption that screw and mixed dislocations are decorated with type I etch pits. On the other hand fig. 5 (c) shows a weak beam dark field image with bragg diffraction vector  $\mathbf{g}=\{11\bar{2}0\}$  which reveals edge and mixed dislocations. The two dislocations on the right side and in the middle (both marked with a white arrows) can also be seen in Fig. 5 (a) and 5 (b) therefore they are mixed dislocations. The left dislocation (black arrow) is only visible in Fig. 5 (b) and (c) thus it can be identified as an edge type dislocation. This is in accordance with our second assumption that edge type dislocations are decorated with type II etch pits. As these etch pits are very flat with a depth of only 1 nm they can not be seen in the TEM image.

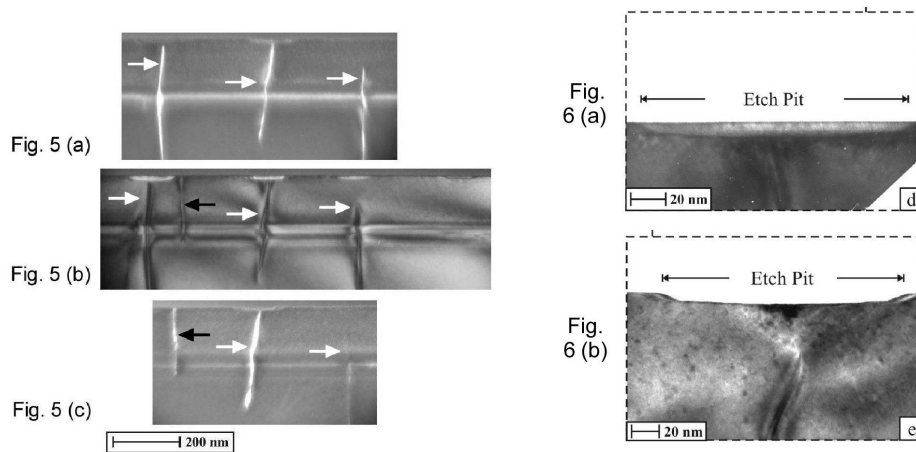


Fig.5: Cross section TEM images of defects with etch pits  
 a) weak beam dark field image, ( $\mathbf{g}=\{0002\}$ )  
 b) bright field image  
 c) weak beam dark field image, ( $\mathbf{g}=\{11\bar{2}0\}$ )

Fig. 6 a), b): Cross section bright field images of type I etch pits

In summary in situ deposited  $\text{SiN}_x$  was used to reduce dislocation density in GaN epilayers on SiC substrates. The growth pressure of the overgrown layer was varied to investigate the influence on smoothing behaviour and defect reduction, whereby the lowest pressure of 70 mbar with a mixture of  $\text{H}_2$  and  $\text{N}_2$  as carrier gas showed the fastest smoothing. The defect density was determined by an etch pit density method which revealed that mainly edge type dislocations could be reduced by a factor of 10. TEM investigations confirm that the two types of etch pits can be related to edge and screw/mixed dislocations. Acknowledgement: This work was partially supported by the German government (BMBF).

## References

- [1] B. Beaumont, Ph. Vennéguès, P. Gibart, *phys. stat. sol. (b)* 227, No. 1, 1–43 (2001)
- [2] S. Haffouz, H. Lahrèche, P. Vennéguès, P. De Mierry, B. Beaumont, F. Omnès, P. Gibart, *Appl. Phys. Lett.* 73, No. 9, 1278 (1998)
- [3] E. Frayssinet, B. Beaumont, J. P. Faurie, P. Gibart, Zs. Makkai, B. Pécz, P. Lefebvre, P. Valvin, *MRS Internet Journal of Nitride Semiconductor Research* Vol. 7, Article 8 (2002)
- [4] P. R Hageman, S. Haffouz, V Kirilyuk, A Grzegorzczuk, P. Larsen, *phys stat sol. (a)* 188, 523 (2001)
- [5] A. Krost, A. Dadgar, *phys. stat. sol. (a)* 194, No. 2, 361 – 375 [2002]
- [6] S. Tanaka, M. Takeuchi, Y. Aoyagi, *Jpn. J. Appl. Phys.* Vol. 39, p. L831 (2000)
- [7] S. Sakai, T. Wang, Y. Morishima, Y. Naoi, *J. Cryst. Growth* 221, 334–337 (2000)
- [8] S. Figge, T. Böttcher, S. Einfeld, D. Hommel, *J. Cryst. Growth* 221, 262 (2000)
- [9] P. Visconti, K. Jones, M. Reshchikov, R. Cingolani, H. Morkoc, *Appl. Phys. Lett.* 77, 3532 (2000)